Astronomy & Astrophysics manuscript no. final2
September 16, 2010

CoRoT light curves of RR Lyrae stars ⋆, ⋆⋆

CoRoT 101128793: long–term changes in the Blazhko effect and excitation of additional modes

E. Poretti[1], M. Paparó[2], M. Deleuil[3], M. Chadid[4], K. Kolenberg[5], R. Szabó[2], J.M. Benkő[2], E. Chapellier[4], E. Guggenberger[5], J.F. Le Borgne[6], F. Rostagni[4], H. Trinquet[4], M. Auvergne[7], A. Baglin[7], L.M. Sarro[8], and W.W. Weiss[5]

[1] INAF – Osservatorio Astronomico di Brera, Via E. Bianchi 46, 23807 Merate (LC), Italy
e-mail: ennio.poretti@brera.inaf.it
[2] Konkoly Observatory of the Hungarian Academy of Sciences, PO Box 67, H-1525 Budapest, Hungary
[3] LAM, UMR 6110, CNRS/Univ. de Provence, 38 rue F. Joliot-Curie, 13388 Marseille, France
[4] Observatoire de la Côte d'Azur, Université Nice Sophia-Antipolis, UMR 6525, Parc Valrose, 06108 Nice Cedex 02, France
[5] Institute of Astronomy, University of Vienna, Türkenschanzstrasse 17, A-1180 Vienna, Austria
[6] Laboratoire d'Astrophysique de Toulouse-Tarbes, Université de Toulouse, CNRS, 14 Av. Edouard Belin, 31400 Toulouse, France
[7] LESIA, Université Pierre et Marie Curie, Université Denis Diderot, Observatoire de Paris, 92195 Meudon Cedex, France
[8] Dpt. de Inteligencia Artificial, UNED, Juan del Rosal 16, 28040 Madrid, Spain

Received, accepted

ABSTRACT

Context. The CoRoT (Convection, Rotation and planetary Transits) space mission provides a valuable opportunity to monitor stars with uninterrupted time sampling for up to 150 days at a time. The study of RR Lyrae stars, performed in the framework of the Additional Programmes belonging to the exoplanetary field, will particularly benefit from such dense, long-duration monitoring.
Aims. The Blazhko effect in RR Lyrae stars is a long-standing, unsolved problem of stellar astrophysics. We used the CoRoT data of the new RR Lyrae variable CoRoT 101128793 (f_0=2.119 d^{-1}, P=0.4719296 d) to provide us with more detailed observational facts to understand the physical process behind the phenomenon.
Methods. The CoRoT data were corrected for one jump and the long-term drift. We applied different period-finding techniques to the corrected timeseries to investigate amplitude and phase modulation. We detected 79 frequencies in the light curve of CoRoT 101128793. They have been identified as the main frequency f_0 and its harmonics, two independent terms, the terms related to the Blazhko frequency f_m, and several combination terms.
Results. A Blazhko frequency f_m=0.056 d^{-1} and a triplet structure around the fundamental radial mode and harmonics were detected, as well as a long-term variability of the Blazhko modulation. Indeed, the amplitude of the main oscillation is decreasing along the CoRoT survey. The Blazhko modulation is one of the smallest observed in RR Lyrae stars. Moreover, the additional modes f_1=3.630 and f_2=3.159 d^{-1} are detected. Taking its ratio with the fundamental radial mode into account, the term f_1 could be the identified as the second radial overtone. Detecting of these modes in horizontal branch stars is a new result obtained by CoRoT.

Key words. Stars: variables: RR Lyrae - stars: oscillations - stars: interiors - stars: individual: CoRoT 101128793 - techniques: photometric

1. Introduction

The pulsation of RR Lyrae stars is paramount for advancing in several fields of stellar physics. Marconi (2009) emphasizes how we can reproduce all the relevant observables of the radial pulsation including only non-local, time-dependent treatment of the convection in nonlinear models. In particular, pulsational models are able to reproduce the correlation between the periods and the absolute magnitudes in the near infrared bands (Bono et al. 2003). The model-fitting technique (Marconi 2009) applied to a sample of RR Lyrae stars in the Large Magellanic Cloud was very useful to fix the problem of the distance scale (Marconi & Clementini 2005). Because they have been observed since the end of the XIXth century, RR Lyrae stars are also promising targets for studying stellar evolution in real time (Le Borgne et al. 2007).

What has not yet been understood in RR Lyrae stars is the Blazhko effect, a periodic modulation of both the amplitudes and phases of the main pulsational mode. Different mechanisms have been proposed to explain the phenomenon: the resonance model between nonradial modes of low degree and the main radial mode (Dziembowski & Mizerski 2004), the oblique pulsator model in which the rotational axis does not coincide with the magnetic axis (Kurtz 1982; Shibahashi 2000), and the action of a turbulent convective dynamo in the lower envelope of the star (Stothers 2006). Kovács (2009) reviews these models and points out why we cannot definitely accept any of these

⋆ The CoRoT space mission was developed and is operated by the French space agency CNES, with participation of ESA's RSSD and Science Programmes, Austria, Belgium, Brazil, Germany, and Spain.
⋆⋆ The CoRoT timeseries, Tables 1 and 2 are available in electronic form at the CDS via anonymous ftp to cdsarc.u-strasbg.fr (130.79.128.5) or via http://cdsweb.u-strasbg.fr/cgi-bin/qcat?J/A+A/vol/page

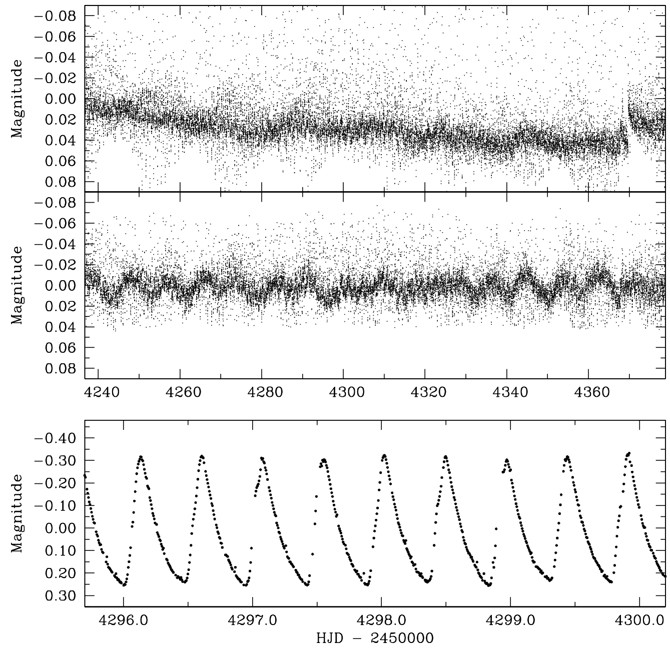

Fig. 1. *Top panel:* the light curve obtained by removing the main frequency and its harmonics from the original data showing a long-term drift and a jump. *Middle panel:* the light curve of the residuals is corrected from the long-term drift and the jump. *Bottom panel:* the final light curve of CoRoT 101128793 is an example of the continuous, excellent quality monitoring of stars in the CoRoT exoplanetary field.

explanations. It seems well–established that Blazhko RR Lyrae stars do not show any strong magnetic field (Chadid et al. 2004; Kolenberg & Bagnulo 2009). The observation of Blazhko RR Lyrae stars was performed with remarkable success by means of extensive ground–based surveys. Well–defined findings (e.g., changes in the Blazhko period, modulation features, systematic changes in the global mean physical parameters, high–order multiplets, long–term changes) have recently been obtained on RR Lyr itself (Kolenberg et al. 2006), MW Lyr (Jurcsik et al. 2008), XZ Cyg (LaCluyzé et al. 2004), RR Gem (Jurcsik et al. 2005; Sódor et al. 2007), and DM Cyg (Jurcsik et al. 2009a).

The Additional Programmes in the exoplanetary science case of the CoRoT (COnvection, ROtation and planetary Transits; Baglin et al. 2006) space mission were focused on specific classes of stars with the aim of supplying a new and powerful tool for deciphering the physical reasons for their variability (Weiss 2006). RR Lyrae stars are being studied in the framework of the international RR Lyrae-CoRoTeam[1]. Preliminary results were presented by Chadid et al. (2009), and the potential of the 150–day continuous monitoring of an RR Lyrae star has been demonstrated by the case of V1127 Aql (Chadid et al. 2010), not previously known as a Blazhko variable. Very high–order modulation sidepeaks were detected, up to the sepdecaplet structure. Additional modes have also been detected and interpreted as nonradial modes or secondary modulation. As the Blazhko effect remains misunderstood in its physical nature, we can look at the CoRoT data as a new opportunity for providing the observational facts we need to shed new light on it.

[1] The dedicated website is http://fizeau.unice.fr/corot.

2. The CoRoT data

CoRoT 101128793≡USNOA2 0900-15089357 (α = $19^h\,26^m\,37^s.33$, δ = $+01^\circ\,13'\,35''.05$, J2000) is a 16th–mag star (V=15.93, $B-V$=+0.89, Deleuil et al. 2009) in the constellation of Aquila. Its variability was discovered during the first Long Run in the centre direction (LRc01), carried out continuously from May 15 to October 14, 2007, i.e., for 142 d. There is no relevant contamination from nearby stars, since the brightest star included in the CoRoT mask is 3.0 mag fainter than CoRoT 101128793 in V light (Deleuil et al. 2009). The exposure time in the CoRoT exoplanetary channel was 512 sec and this time remained constant all over the LRc01. Thanks to its very high duty cycle, CoRoT collected 23922 data points, and the spectral window is free from any relevant alias structure. The star was classified as an RR Lyrae variable by the "CoRoT Variability Classifier" automated supervised method (Debosscher et al. 2009) and then confirmed by human inspection of the light curve. CoRoT 101128793, located close to the direction of the galactic centre, is therefore heavily reddened.

The absolute CoRoT photometry is affected by jumps, outliers, and a long-term drift. It is very hard to detect jumps in the original data of an RR Lyrae variable, since they have a small amplitude (few 0.01-mag) and are not discernible in a light curve having an amplitude of several tenths of a magnitude. As a matter of fact, we could detect a jump of 0.032 mag at JD 2454369.7 only a posteriori, after having performed the preliminary frequency analysis of the original data. Indeed, only the residuals obtained by subtracting the main frequency f_0 and its harmonics from the original CoRoT data clearly show the jump. We re-aligned the whole dataset after removing the few corrupted measurements on the jump (Fig. 1, top and middle panels).

In addition to the jump, some oscillations and a continuous drift are clearly visible in the top panel of Fig. 1. The oscillations have a stellar origin (see Sect. 3.2), but the drift is an instrumental effect (Auvergne et al. 2009), so it should be removed before performing the frequency analysis. Different detrending algorithms can be used, based on moving means or polynomial fits. After several trials, we removed the drift by calculating the mean magnitudes of the least–squares fits of four consecutive cycles (i.e., 1.88 d). The main frequency and its harmonics were used, as in the previous step. At that point, the value of the mean magnitude was interpolated at the time of each observation and then subtracted from the original data. During this analysis we also removed the most obvious outliers. The final CoRoT timeseries is available in electronic form at the CDS. The re-aligned, de-jumped light curve disclosed the multiperiodic behaviour of CoRoT 101128793: continuous oscillations are clearly visible in the light curve prewhitened with f_0 and harmonics (Fig. 1, middle panel) and in the light curve of the original data (a portion is shown in Fig. 1, bottom panel).

The subsequent frequency analysis was performed by using different packages such as Period04 (Lenz & Breger 2005), MuFrAn (Kolláth 1990), and the iterative sine–wave fitting (Vaniĉek 1971). The different algorithms led to the same results with only marginal differences at higher orders. We present here the results of the iterative–sine wave fitting, with a complementary frequency refinement obtained by means of the MTRAP algorithm (Carpino et al. 1987).

The realigned dataset was first analysed to search for the effects of the orbital frequency. Several frequencies were found at the orbital frequency f_{orb}=13.97 d^{-1} and harmonics. Moreover, the term f_{sid}=1.0027 d^{-1} was found. This perturbation comes from the passage of the satellite over the South Atlantic

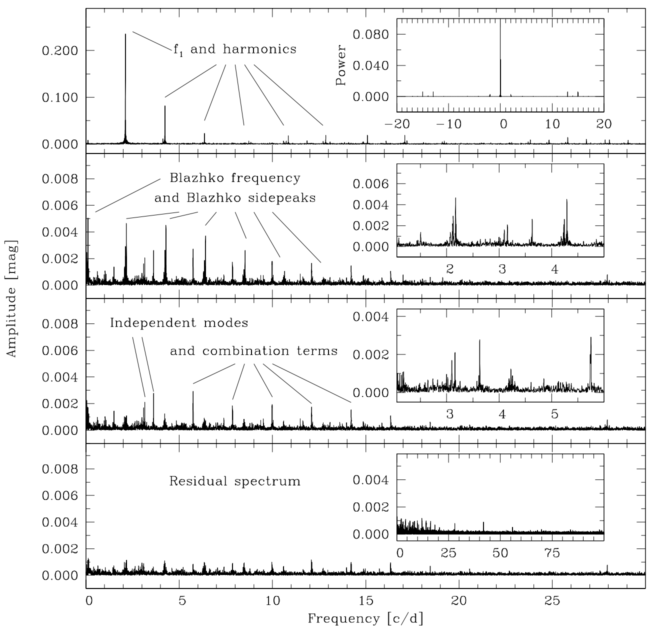

Fig. 2. Subsequent steps in the detection of frequencies in the amplitude spectra of CoRoT 101128793.

Anomaly (SAA). Since it occurs twice a day, the harmonic $2f_{sid}$ is much stronger than f_{sid}, which corresponds to the passage of the satellite over the SAA on the same side of the Earth with respect to the Sun. The effects of these passages on the onboard instrumentation are described by Auvergne et al. (2009). They originate frequencies at

$$f_{o,s} = k_1\ f_{orb} \pm k_2 f_{sid} \tag{1}$$

with $0 \leq k_1 \leq 7$ and $-4 \leq k_2 \leq 4$. The strongest terms are 27.94 and 41.91 d^{-1}, i.e., $(k_1, k_2) = (2,0)$ and (3,0), respectively. The usually adopted technique of prewhitening the input data with the frequencies $f_{o,s}$ did not correct for the instrumental effects in a satisfactory way. The orientation of the CoRoT orbital plane with respect to the Earth–Sun line continuously changed over the course of the long run. Therefore, the environmental conditions (e.g., the eclipse effects on the electronics units, the eclipse durations, the difference in the Earth's albedo of the overflown regions; see Sect. 3 in Auvergne et al. 2009) are affecting the CoRoT photometry in a complicated way.

3. The frequency content

By using the packages previously mentioned, we identified 79 components of stellar origin, in addition to the $f_{o,s}$ frequencies and to the spurious peaks at very low frequencies, i.e., residuals of the long–term drift of the sensitivity drift of the CCDs. They can be divided into four categories:

1. the main frequency f_0 and its harmonics;
2. the terms related to the Blazhko frequency f_m;
3. other independent terms;
4. the combination terms.

Figure 2 describes the different steps in the frequency detection. The spectrum in the top panel brings out the main frequency f_0=2.119 d^{-1} and its harmonics. The spectral window (inserted box) is almost free of aliases, and the peaks located at f_{orb} and $2f_{sid}$ are too low to produce any significant effect. When f_0 and harmonics are removed, the couple of sidepeaks ($f_0 \pm f_m$, with f_m=0.056 d^{-1}) due to the Blazhko effect becomes the most prominent structure (second panel, the zoom around f_0 and $2f_0$ is shown in the inserted box).

The most intriguing peaks stand out in the region 3 – 4 d^{-1} after subtracting the Blazhko sidepeaks (third panel and inserted box). The highest peaks in the third panel of Fig. 2 are at f_1=3.157 d^{-1} and f_2=3.630 d^{-1}. They show linear combination with f_0 and harmonics and are therefore intrinsic to the RR Lyrae star. They provide evidence of excited modes other than the fundamental radial mode f_0.

The residual spectrum does not show any other structure, except an excess of signal still centred on the largest amplitude modes and on the orbital frequencies of the satellite (Fig. 2, bottom panel). After removing the 79 frequencies, the average noise level resulted in 7×10^{-5} mag in the 0-100 d^{-1} region of the residual spectrum (inserted box in Fig. 2, bottom panel). The lowest detected amplitude among the 79 frequencies led to 0.36 mmag, i.e., 5 times the level of the overall final noise. We note that at each step of the process in frequency detection we calculated the local noise centred on the detected peak, and we always got SNR>3.5. This threshold was retained to accept a combination term, while independent terms have much higher SNR (17.45 and 9.25 for f_1 and f_2, respectively).

The final solution of the CoRoT light curve was calculated by means of a cosine series (T_0=2454308.2168) and their least–squares parameters, together with the local SNRs, are listed in Table 1. The listed values of the frequencies are corresponding to the highest peaks in the amplitude spectrum. The values calculated from the four independent frequencies and the identification listed in the last column of Table 1 (the so-called locked solution, obtained by using the MTRAP algorithm, Carpino et al. 1987) are generally in excellent agreement (f_0=2.118977, f_1=3.630499, f_1=3.156776, and f_m=0.00550 d^{-1}). The observed discrepancies are probably due to the non–equidistance of the triplet structures and to other terms hidden in the residual noise. As an example, a third independent frequency is probably present close to 3.00 d^{-1}, but we cannot identify it unambiguously. If this f_3 term were real, then some combination terms should be changed by substituting, e.g., $2f_1$ with $2f_0+f_4$. The solution with all independent frequencies gives the same residual rms of the solution with the locked frequencies (0.01006 and 0.01100 mag, respectively). These values are mostly affected by the residual peaks described above.

3.1. The main f_0 term and its harmonics

The light curve on the f_0 term is very asymmetric (Fig. 3, upper curve in the top panel) and harmonics up to $13f_0$ are significant. Their amplitudes are not monotonically decreasing: the amplitude of $6f_0$ is larger than for $5f_0$, and that of $11f_0$ is larger than for $10f_0$, just before the final decline (Fig. 3, left panel in the bottom row). Indeed, the light curve of CoRoT 101128793 shows a couple of particularities, i.e., the bump near the minimum often observed in RRab stars and a change in slope on the rising branch. They are not very pronounced, but still discernible in the light curve (Fig. 1, bottom panel). The fit of these small particularities requires a more relevant contribution from the highest harmonics than in the case of smooth light curves. Moreover, the change in slope does not repeat in a regular way, since the plot of the residuals (Fig. 3, lower curve in the top panel) shows a wide spread in this phase interval. The non–

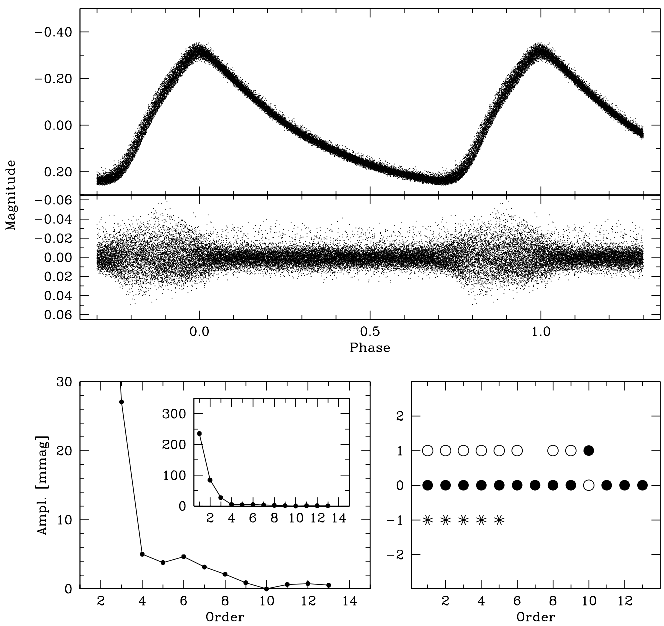

Fig. 3. *Upper panel:* The CoRoT data folded with f_0, original (top) and after subtracting the 79 frequencies (bottom). *Left panel, lower row:* The amplitudes of the $n\ f_0$ terms. *Right panel, lower row:* The observed triplet structure around $n\ f_0$ terms. The filled circles indicate the component with the greatest amplitude in the triplet, the empty circles the second in amplitude, the star the third.

white distribution of the photometric residuals is the cause of the small bunches of frequencies observed in the residual spectrum. The Blazhko variables RR Gem and DM Cyg show the same light curve shape and the same residual distribution as CoRoT 101128793 (Jurcsik et al. 2005, 2009a).

The measurements around the maximum and minimum brightnesses were fitted by means of a least-squares polynomial. We obtained the ephemeris

$$\mathrm{Max} = \mathrm{HJD}\ \ 2454236.6752\ \ +0.4719296\ \mathrm{xE}$$
$$\pm 0.0003\ \ \pm 0.0000018$$

when fitting the times of maxima (Table 2) by means of a least–squares line. The O-C values (differences between the observed and calculated times of maxima) were determined by using this ephemeris.

3.2. The Blazhko frequency f_m

As suggested by the residuals after subtracting the main oscillation (Fig. 1, middle panel), there is a periodic change in the shape of the light curve, and this change defines the Blazhko effect. The Blazhko effect translates into symmetric sidepeaks of f_0 and its harmonics in the frequency domain (second panel in Fig. 2). In the case of CoRoT 101128793, the sidepeaks are $n\ f_0 \pm f_m$ triplets (Fig. 3, right panel in the bottom row).

We obtained an independent confirmation of the Blazhko frequency from the magnitudes at the maximum brightness (see above) and from the application of the analytic signal method (Kolláth et al. 2002). The magnitudes at maximum oscillate in a peak-to-peak interval of 0.06 mag (Fig. 4, top panel): the power spectrum unambiguously identifies f_m=0.056 d^{-1} (Fig. 4, bottom panel). The instantaneous amplitudes and frequencies also vary with f_m (Fig. 4, middle panel). The period variations, and consequently the O-C range, are very small. As a matter of fact, CoRoT 101128793 shows the smallest period variation among the CoRoT RRab stars (see Fig. 2 in Szabó et al. 2009). Since the Blazhko effect is more evident in amplitude than in phase, the cycle–to–cycle variations in the light curve are undetectable when folding the data over f_0, also considering the perfect coverage in phase ensured by the CoRoT observations. The Blazhko effect just causes a wider spread of the points, while the curve apparently remains very regular (Fig. 3, top panel). The Blazhko effect of CoRoT 101128793 seems to be particular since the harmonic $2 f_m$ has an amplitude greater than f_m (Table 1 and middle panel of Fig. 1). This particularity could reflect the different forms in which the Blazhko effect can occur (see Table 1 in Szabó et al. 2009). However, we should also consider that the frequency and amplitude values of f_m and $2 f_m$ could be affected by the slightly different separations between the sidepeaks of the triplets (Table 1) and by the correction of the low–frequency drift.

We observe a peak close to zero (Fig. 4, bottom panel) in the power spectrum of the magnitudes at maximum. This suggests that there is a very long–term variation, on a timescale longer than covered by the CoRoT data. The complicated behaviour of the light curve is made clear by the comparison between maxima and minima (Fig. 4, upper panel). The range in the magnitudes at minimum is about half that at the maximum. Also the amplitudes of the f_0 component (calculated both as instantaneous values and by subdividing the timeseries in pulsational cycles) show the decreasing trend underlying the Blazhko periodicity (Fig. 4, middle panel).

The long–term change is a further complication of the frequency analysis (Benkő et al. 2009; Szeidl & Jurcsik 2009). Together with the change in slope on the rising branch, it causes the peaks around f_0 and its harmonics in the residual spectrum (Fig. 2, bottom panel).

3.3. The independent terms

3.3.1. f_1=3.630 d^{-1}

The first peak not related to f_0 and f_m is found at f_1=3.630 d^{-1}. The light curve related to this periodicity is slightly asymmetrical, since we found a small-amplitude first harmonic $2 f_1$. It also shows several combination terms with $n\ f_0$ and $n\ f_0 \pm f_m$. However, f_1 is not affected by the Blazhko effect, since we did not detect terms of the form $f_1 \pm f_m$.

The ratio f_0/f_1=0.584 is very close to what is expected between the fundamental radial mode and the second overtone. To verify this possibility from a theoretical point of view, we computed linear RR Lyrae model grids on an extremely large parameter space (L=40, 50, 60 and 70 L$_\odot$, M=0.50–0.80 M$_\odot$ with ΔM=0.05 M$_\odot$, $T_{\rm eff}$=5000–8000 K, $\Delta T_{\rm eff}$=100 K, Z =0.001, 0.003, 0.01, 0.02 and 0.04). The other adopted parameters were standard RR Lyrae parameters (see Szabó et al. 2004). Nonlinearity introduces a negligible difference in the periods and period ratios. The Petersen diagram for different metallicities is shown in Fig. 5. The period ratio is fully compatible with an identification of f_1 as the second radial overtone. In such a case, the models suggest a Z-metallicity of 0.002-0.004. Assuming a ratio of 0.74 between fundamental and first overtone radial modes, the latter should be around 2.863 d^{-1}, but the frequency spectrum does not show any significant peak at this value.

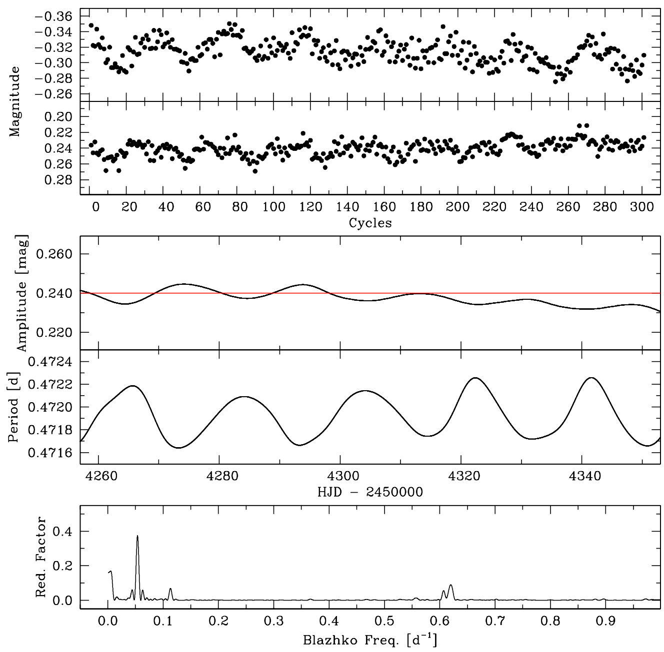

Fig. 4. Evidence of the long–term variations in the CoRoT 101128793 light curve. *Top panel:* The magnitudes at maximum (upper curve) and minimum (lower curve) brightness in the different cycles. *Middle panel:* The amplitudes of the f_0 component (upper curve) and the period values (lower curve). Reference line is displayed to show the long term variation in amplitude. *Bottom panel:* The power spectrum of the magnitudes at maximum brightness.

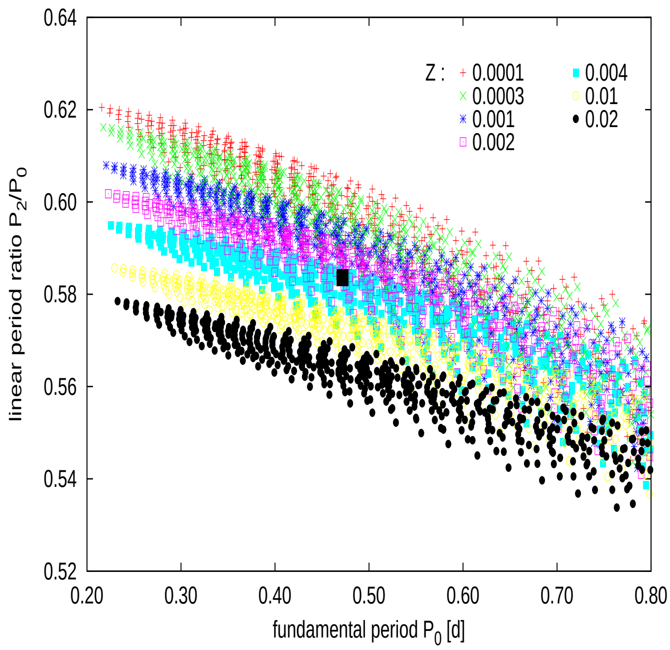

Fig. 5. Petersen diagram based on linear convective RR Lyrae models. The symbols denote different metallicities. The black square shows the position of CoRoT 101128793, assuming that the frequency f_2 is the second overtone radial mode.

3.3.2. f_2=3.159 d^{-1}

The amplitude of f_2=3.159 d^{-1} is only a bit smaller than that of f_1 (0.0021 and 0.0028 mag, respectively) and at the same level of that of the $8f_0$ harmonic. The ratio f_2/f_0=1.4908~3/2 could be the signature of the period doubling bifurcation (Moskalik & Buchler 1990) first noticed in some RR Lyrae stars observed with *Kepler* (Kolenberg et al. 2010).

Another characteristic of f_2 is to be flanked by a Blazhko frequency at f_2-f_m. This occurrence can have different explanations : *i)* the Blazhko variability also affects f_2; *ii)* it is a coincidence, and f_2 and f_2-f_m are actually two independent modes; *iii)* f_2-f_m is a mere combination term, such as the difference between f_0+f_2 and f_0+f_m. We can try to disentangle the matter by examining the three possibilities. If f_2 shows the Blazhko effect, it is strange that we do not detect f_2+f_m since we expect the sum term to have an amplitude greater than the difference term (see Fig. 3, right panel in the bottom row). The coincidence is also improbable, since the frequency spectrum is not very rich. The resonance mechanism is possible, but that it involves the Blazhko term makes it a very particular case. Finally, combination terms with $n\,f_0$, $n\,f_0\pm f_m$, and f_1 are detected. In particular, we found unusual combinations, such as $f_0+f_1+f_2$ and $f_0+f_m+f_1+f_2$, and they display a good SNR (5.4 and 4.6, respectively). Therefore, the hypothesis of a particular combination term seems the most plausible.

4. Discussion

The continuous, long monitoring offered by space photometry is a new observational tool to understand the pulsational behaviour of RR Lyrae stars. Through such data, cycle–to–cycle variations can be clearly pointed out. Indeed, the Blazhko modulation of CoRoT 101128793 is one of the smallest ever observed in RR Lyrae stars (Jurcsik et al. 2009b).

4.1. The Blazhko effect

CoRoT data already demonstrated that the Blazhko cycle of V1127 Aql is changing on a timescale of 143 d: the shift is much more evident in time than in magnitude (see Fig. 14 in Chadid et al. 2010). The Blazhko effect of CoRoT 101128793 is much smaller than that of V1127 Aql (0.06 mag vs. 0.35 mag in the full range of magnitudes at maximum, 0.02 p vs. 0.17 p in the phases of maximum).

Notwithstanding this small effect, the trend observed in the magnitudes at maximum and at minimum (Fig. 4, upper panel) supports a long–term change. The best observational evidence for a long–term change in the Blazhko period is given by RR Lyr itself. Ground–based photometry collected on several decades shows a decrease from 40.8 d to 38.8 d (Kolenberg et al. 2006). The modulation amplitude of RR Gem was also subjected to strong variations from the undetectable level (less than 0.04 mag in maximum brightness) to about 0.20 mag on a time baseline of 70 years (Sódor et al. 2007). In the case of the Blazhko effect of MW Lyrae (f_m=0.060 d^{-1}), Jurcsik et al. (2008) put in evidence secondary peaks around the main pulsation terms separated by a periodicity comparable with the time baseline, tentatively ~500 d. Therefore, it seems that long–term changes are occurring in Blazhko RR Lyrae variables, and they can be detected when monitored in an intensive and/or continuous way.

4.2. The excitation of additional modes

The case of CoRoT 101128793 supplies new evidence of the excitation of additional modes in RR Lyrae stars. The two frequencies f_1 and f_2 are not related with the Blazhko or another modulation, as it could be for V1127 Aql (Chadid et al. 2010). The frequency f_1 could be typified as the second overtone radial mode, while the nature of f_2 is still unclear. We immediately note that also in the case of V1127 Aql we found frequency ratios compatible with that between fundamental and second overtone radial modes, i.e., 2.8090/4.8254=0.582, and with the possible period doubling bifurcation, i.e., 4.1916/2.8090=1.492. Moreover, the frequency values f_1 and f_2 are in the same interval of the nine additional modes detected in the frequency spectrum of V1127 Aql (3.64–4.82 d^{-1}).

It is interesting to revisit the results obtained by Jurcsik et al. (2008) on MW Lyr. Those authors identified four frequencies in the 3.27–6.78 d^{-1} interval (3.2701, 4.2738, 5.7847, and 6.7885 d^{-1})[2] as combination terms having the form $n\,f_0 \pm 12.5\,f_m$ (where f_0=2.5146 d^{-1} is the main pulsation mode and f_m=0.0604 d^{-1} the Blazhko frequency). Since the 12.5 f_m spacing remains unexplained, we propose an alternative solution based on the additional modes f_1=3.2701 d^{-1} and f_2=4.2738 d^{-1} and the combination terms $f_0 + f_1$=5.7847 d^{-1} and $f_0 + f_2$=6.7884 d^{-1}. We find for the third time a frequency ratio (f_0/f_2=0.588) that could be explained with the ratio between the fundamental and the second overtone radial modes.

These mode identifications are a new contribution to the debate on the excitation of the second overtone in RR Lyr stars (e.g., Alcock et al. 1996; Walker & Nemec 1996; Kaluzny et al. 2000; Soszyński et al. 2003; Olech & Moskalik 2009). We also note that the excitation of non-consecutive radial modes would be a new result for RR Lyr stars, so far sporadically observed in Cepheids (Soszyński et al. 2008).

5. Conclusions

The second detailed analysis of the CoRoT data on RR Lyrae variables allowed us to advance in the definition of their pulsational characteristics. It is confirmed that the Blazhko effect can span different ranges in the variations, both absolute and relative, of the amplitude and phase modulations. Moreover, there is new evidence that the Blazhko period is subjected to long–term variations, as can be directly detected from the consecutive cycles observed in the CoRoT LRc01. The mechanisms invoked to explain the Blazhko effect should reproduce "the strictly regular behavior of the modulation observed in many Blazhko stars" (Jurcsik 2009). This requirement should now be reconsidered in a slightly different way. The real mechanism must be able to reproduce both the regular structure of the sidepeaks in the frequency spectra and the observed variability on a long–term scale. In this context, it can be useful to stress that CoRoT 101128793, similar to DM Cyg (Jurcsik et al. 2009a) and RR Gem (Jurcsik et al. 2005), shows a bump on the rising branch of the light curve. These bumps are probably connected with hypersonic shock waves (Chadid et al. 2008), and the spreading of the residuals suggests a link between pulsation and atmosphere dynamics. More precisely, this could be the clue to an interaction between the Blazhko phenomenon and the atmosphere's dynamics (Guggenberger & Kolenberg 2006), since monoperiodic RR Lyrae stars also have very regular light curves in the presence of this bump (Poretti 2001).

The other relevant result disclosed by the CoRoT data is the excitation of additional modes. A reanalysis of the V1127 Aql and MW Lyr cases seems to indicate that there is a narrow frequency interval where a few modes are excited. The recurrence of the ratio 0.58–0.59 between one of these modes and the fundamental radial mode suggests the possibility of the (preferred) excitation of the second overtone. The possible interplay between this type of double–mode pulsation and the Blazhko effect deserves further theoretical investigation. The Blazhko effect does not modulate the f_1 term and this is particularly relevant in this scenario. Moreover, CoRoT detected other very significant peaks in the oscillation spectra of V1127 Aql and CoRoT 101128793, thus disclosing the evidence that nonradial modes are excited in horizontal branch stars. The theoretical prediction of these modes is the new challenge to the pulsation models of RR Lyrae stars launched by CoRoT.

Acknowledgements. This research has made use of the Exo-Dat database, operated at LAM-OAMP, Marseille, France, on behalf of the CoRoT/Exoplanet programme. MC thanks F. Baudin and J. Debosscher for their help on the data reduction. JMB, MP, and RSz acknowledge the support of the ESA PECS projects No. 98022 & 98114. KK and EG acknowledge the projects FWF T359 and FWF P19962, and EP the Italian ESS project (contract ASI/INAF/I/015/07/0, WP 03170) for financial support.

References

Alcock, C., Allsman, R.A., Axelrod, T.S., et al. 1996, AJ, 111, 1146
Auvergne, M., Bodin, P., Boisnard, L., et al. 2009, A&A, 506, 411
Baglin, A., Auvergne, M., Barge, P., et al. 2006, in "The CoRoT Mission, Pre-Launch Status, Stellar Seismology and Planet Finding", M. Fridlund, A. Baglin, J. Lochard, L. Conroy Eds., ESA SP-1306 (ESA Publications Division, Nordwijk, Netherlands), p. 33
Benkő, J. M., Paparó, M., Szabó, R., et al. 2009, in IAP Conf. Ser., Stellar Pulsation: Challanges for Theory and Observation, J. A. Guzik & P. Bradley Eds., 1170, 273
Bono, G., Caputo, F., Castellani, V., et al. 2003, MNRAS, 344, 1097
Carpino, M., Milani, A., & Nobili, A.M. 1987, A&A, 181, 182
Chadid, M., Baglin, A., Benkő, J., et al. 2009, in IAP Conf. Ser., Stellar Pulsation: Challanges for Theory and Observation, J. A. Guzik & P. Bradley Eds., 1170, 235
Chadid, M., Benkő, J.M., Szabó, R., et al. 2010, A&A, 510, A39
Chadid, M., Vernin, J., & Gillet, D. 2008, A&A, 491, 537
Chadid, M., Wade, G. A., Shorlin, S. L. S., & Landstreet, J. D. 2004, A&A, 413, 1087
Debosscher, J., Sarro, L. M., López, et al. 2009, 506, 519
Deleuil, M., Meunier, J. C., Moutou, et al. 2009, AJ, 138, 649
Dziembowski, W.A., & Mizierski, T. 2004, Acta Astron., 54, 363
Guggenberger, E., & Kolenberg, K. 2006, CoAst, 148, 21
Jurcsik, J. 2009, in IAP Conf. Ser., Stellar Pulsation: Challanges for Theory and Observation, J. A. Guzik & P. Bradley Eds., 1170, 286
Jurcsik, J., Hurta, Zs., Sódor, Á., et al. 2009a, MNRAS, 397, 350
Jurcsik, J., Sódor, Á., Hurta, Zs., et al. 2008, MNRAS, 391, 164
Jurcsik, J., Sódor, Á., Szeidl, B., et al. 2009b, MNRAS, 400, 1006
Jurcsik, J., Sódor, Á., Váradi, M., et al. 2005, A&A, 430, 104
Kaluzny, J., Olech, A., Thompson, I., et al. 2000, A&AS, 143, 215
Kolenberg, K., & Bagnulo, S. 2009, in IAP Conf. Ser., Stellar Pulsation: Challanges for Theory and Observation, J. A. Guzik & P. Bradley Eds., 1170, 281
Kolenberg, K., Smith, H.A., Gazeas, K.D., et al. 2006, A&A, 459, 577
Kolenberg, K., Szabó, R., Kurtz, D., et al. 2010, ApJ, 713, L198
Kolláth, Z., Buchler, J., Szabó, R., & Csubry, Z. 2002, A&A, 385, 932
Kolláth, Z. 1990, Occ. Tech. Notes Konkoly Obs., Budapest, No. 1
Kovács, G. 2009, in IAP Conf. Ser., Stellar Pulsation: Challanges for Theory and Observation, J. A. Guzik & P. Bradley Eds., 1170, 261
Kurtz, D.W. 1982, MNRAS, 200, 497
LaCluyzé, A., Smith, H.A., Gill, E.-M., et al. 2005, AJ, 127, 1653
Le Borgne, J.F., Paschke, A., Vandenbroere, J., et al. 2007, A&A, 476, 307
Lenz, P., & Breger, M. 2005, CoAst, 146, 53

[2] We note that there is a 1 d^{-1} spacing between the terms of the first couple and between those of the second one. This spacing is always a bit suspicious for observations collected mostly from one site, but we consider the frequency detection performed by Jurcsik et al. (2008) as a well-established one.

Marconi, M. 2009, in IAP Conf. Ser., Stellar Pulsation: Challanges for Theory and Observation, J. A. Guzik & P. Bradley Eds., 1170, 223
Marconi, M., & Clementini, G. 2005, AJ, 129, 2257
Moskalik, P., & Buchler, J.R. 1990, ApJ, 355, 590
Olech, A., & Moskalik, P. 2009, Acta Astron., 494, L17
Poretti, E. 2001, A&A, 371, 986
Shibahashi, H. 2000, in "The Impact of Large-Scale Surveys on Pulsating Star Research", L. Szabados & D. Kurtz Eds., ASP Conf. Series, 203, 299
Sódor, Á., Szeidl, B., & Jurcsik, J. 2007, A&A, 469, 1033
Soszyński, I., Udalski, A., Szymanski, M., et al. 2003, Acta Astron., 53, 93
Soszyński, I., Poleski, R., Udalski, A., et al. 2008, Acta Astron., 58, 163
Stothers, R.B. 2006, ApJ, 652, 643
Szabó, R. Kolláth, Z., & Buchler, J. R. 2004, A&A, 425, 627
Szabó, R., Paparó, M., Benkő, J., et al. 2009, in IAP Conf. Ser., Stellar Pulsation: Challanges for Theory and Observation, J. A. Guzik & P. Bradley Eds., 1170, 291
Szeidl, B., & Jurcsik, J. 2009, CoAst, 160, 17
Vaniĉek, P. 1971, Ap&SS 12, 10
Walker, A.R., & Nemec, J.M. 1996, AJ, 112, 2026
Weiss, W.W. 2006, in "The CoRoT Mission, Pre-Launch Status, Stellar Seismology and Planet Finding", M. Fridlund, A. Baglin, J. Lochard, L. Conroy Eds., ESA SP-1306 (ESA Publications Division, Nordwijk, Netherlands), p. 93

Table 1. Fourier amplitudes, phases, signal-to-noise ratio, and identification of the frequencies detected in the CoRoT data of the star CoRoT 101128793.

Frequency [d^{-1}]	Amplitude [mag]	Phase [0,2π]	SNR	ID
Main frequency and harmonics				
2.1189511	0.235160	0.2021	83.170	f_0
4.2379699	0.083192	4.4638	81.173	$2f_0$
6.3567948	0.025942	2.5909	69.957	$3f_0$
8.4750872	0.003859	0.9586	25.783	$4f_0$
10.5955076	0.004677	2.0603	26.972	$5f_0$
12.7142172	0.005179	0.1356	32.102	$6f_0$
14.8329821	0.003394	4.4305	24.368	$7f_0$
16.9521809	0.002134	2.1695	16.597	$8f_0$
19.0711250	0.000924	0.0034	9.907	$9f_0$
21.1895828	0.000362	2.6349	5.089	$10f_0$
23.3090458	0.000650	0.1582	8.902	$11f_0$
25.4280815	0.000657	4.1858	9.371	$12f_0$
27.5470715	0.000427	2.1154	5.925	$13f_0$
Blazhko modulation				
0.0557860	0.002250	3.5242	11.027	f_m
0.1130970	0.005032	2.0600	21.865	$2f_m$
Modulation triplet frequencies				
2.0706120	0.001003	4.3047	6.254	$f_0 - f_m$
2.1719539	0.004580	5.3412	17.976	$f_0 + f_m$
4.1836190	0.000864	4.5330	5.714	$2f_0 - f_m$
4.2913609	0.004452	2.8623	22.069	$2f_0 + f_m$
6.3063798	0.000914	1.7760	7.603	$3f_0 - f_m$
6.4105959	0.003799	1.2182	19.970	$3f_0 + f_m$
8.4165525	0.000603	2.4485	5.293	$4f_0 - f_m$
8.5297117	0.002889	6.1076	18.665	$4f_0 + f_m$
10.5445929	0.000403	4.8041	3.957	$5f_0 - f_m$
10.6492252	0.001437	4.1638	10.704	$5f_0 + f_m$
12.7694759	0.000618	2.3372	6.028	$6f_0 + f_m$
17.0050011	0.000589	2.2322	7.826	$8f_0 + f_m$
19.1245899	0.000586	0.3344	6.950	$9f_0 + f_m$
21.2440968	0.000399	4.5191	5.034	$10f_0 + f_m$
Additional terms identified as independent modes				
3.1588659	0.002119	2.9665	9.251	f_2
3.6308789	0.002844	1.0416	17.450	f_1
Linear combinations between additional terms and f_0, with or without f_m				
0.5557140	0.000579	1.4162	3.590	$2f_0 - f_m - f_1$
0.6137300	0.000967	4.3577	5.458	$2f_0 - f_1$
0.9815810	0.000673	5.9134	4.446	$f_2 - f_0 - f_m$
1.0310810	0.000907	4.4587	5.680	$2f_0 - f_m - f_2$
1.0892100	0.000625	0.2036	4.373	$2f_0 - f_2$
1.1364660	0.000529	0.0723	4.307	$2f_0 + f_m - f_2$
1.5060490	0.001430	3.0864	9.914	$f_1 - f_0$
2.7380049	0.000817	0.5867	4.017	$3f_0 - f_1$
3.0997059	0.001693	2.0588	7.816	$f_2 - f_m$
3.2565880	0.000691	5.0736	4.663	$3f_0 + f_m - f_2$
4.8528800	0.000808	4.6690	5.310	$4f_0 - f_1$

Table 1. continued.

Frequency $[d^{-1}]$	Amplitude [mag]	Phase $[0,2\pi]$	SNR	ID
5.1331830	0.000699	1.0265	4.088	$2f_1 - f_0$
5.2227440	0.000559	0.6052	4.755	$f_0 - f_m + f_2$
5.2794271	0.000596	6.1065	4.413	$f_0 + f_2$
5.3320541	0.000404	0.1849	3.706	$f_0 + f_m + f_2$
5.3743072	0.000564	2.6932	5.144	$4f_0 + f_m - f_2$
5.6918921	0.000502	1.0524	3.988	$f_0 - f_m + f_1$
5.7496319	0.002907	5.7320	18.811	$f_0 + f_1$
6.9680071	0.000622	3.9101	4.517	$5f_0 - f_1$
7.2510352	0.000450	3.3737	3.567	$2f_1$
7.3422809	0.000408	6.1252	3.540	$2f_0 - f_m + f_2$
7.3839550	0.000509	2.9947	4.455	$5f_0 - f_m + f_2$
7.3946028	0.001058	5.1992	8.021	$2f_0 + f_2$
7.8696060	0.001498	3.8452	10.900	$2f_0 + f_1$
8.9037333	0.000488	1.7403	5.396	$f_0 + f_1 + f_2$
8.9577160	0.000431	3.1197	4.556	$f_0 + f_m + f_1 + f_2$
9.0911274	0.000523	1.7513	4.075	$6f_0 - f_1$
9.3717070	0.000840	2.8583	5.426	$f_0 + 2f_1$
9.4592342	0.000536	4.5554	4.219	$3f_0 - f_m + f_2$
9.5042696	0.000520	1.3052	4.413	$6f_0 - f_m - f_2$
9.5122747	0.001021	3.4523	7.300	$3f_0 + f_2$
9.9870539	0.002025	2.1231	14.298	$3f_0 + f_1$
10.0394773	0.000660	4.7210	5.748	$3f_0 + f_m + f_1$
11.4905624	0.000896	0.9388	6.940	$2f_0 + 2f_1$
11.5774755	0.000494	2.9245	4.427	$4f_0 - f_m + f_2$
11.6231632	0.000689	6.1547	6.080	$7f_0 - f_m - f_2$
11.6310463	0.000901	1.6964	7.590	$4f_0 + f_2$
12.1040316	0.001536	0.2982	12.757	$4f_0 + f_1$
12.1594105	0.000564	3.3520	5.916	$4f_0 + f_m + f_1$
13.6098433	0.000621	5.4812	5.738	$3f_0 + 2f_1$
13.7422590	0.000518	4.7605	5.055	$8f_0 - f_m - f_2$
13.7495470	0.000543	5.8919	5.436	$5f_0 + f_2$
14.2228832	0.001424	4.3996	12.419	$5f_0 + f_1$
14.2800894	0.000424	1.1744	5.263	$5f_0 + f_m + f1$
15.8649635	0.000590	3.1909	6.673	$9f_0 - f_m - f_2$
16.3416233	0.001096	2.4098	11.503	$6f_0 + f_1$
18.4694328	0.000364	2.2220	4.735	$7f_0 + f_1$
20.5785885	0.000401	5.4055	5.082	$8f_0 + f_1$

Table 2. Times, magnitudes, O–Cs of the maxima observed in the light curve of CoRoT 101128793.

Cycle [E]	Times of maximum [HJD-2450000]	Magnitude	O–C [d]	Cycle [E]	Times of maximum [HJD-2450000]	Magnitude	O–C [d]
1	4237.1460	–0.3481	–0.0011	152	4308.4114	–0.3176	0.0039
2	4237.6211	–0.3223	0.0020	153	4308.8767	–0.3193	–0.0026
3	4238.0891	–0.3212	–0.0019	154	4309.3486	–0.3275	–0.0027
4	4238.5593	–0.3433	–0.0036	155	4309.8227	–0.3256	–0.0005
5	4239.0325	–0.3235	–0.0023	156	4310.2949	–0.3154	–0.0002
6	4239.5027	–0.3198	–0.0040	157	4310.7649	–0.3407	–0.0022
7	4239.9727	–0.3320	–0.0060	158	4311.2380	–0.3426	–0.0009
8	4240.4509	–0.3178	0.0003	159	4311.7131	–0.3095	0.0022
9	4240.9238	–0.2999	0.0013	160	4312.1831	–0.3143	0.0003
10	4241.3940	–0.3041	–0.0004	161	4312.6543	–0.3347	–0.0004
11	4241.8623	–0.3200	–0.0040	162	4313.1284	–0.3271	0.0018
12	4242.3445	–0.2937	0.0062	163	4313.5996	–0.3015	0.0010
13	4242.8106	–0.2937	0.0004	164	4314.0696	–0.3206	–0.0009
14	4243.2808	–0.2988	–0.0014	165	4314.5408	–0.3260	–0.0017
15	4243.7578	–0.2943	0.0038	166	4315.0198	–0.3010	0.0054
16	4244.2319	–0.2883	0.0060	167	4315.4849	–0.3081	–0.0014
17	4244.6968	–0.2926	–0.0011	168	4315.9570	–0.3149	–0.0012
18	4245.1719	–0.3093	0.0021	169	4316.4329	–0.3228	0.0027
19	4245.6462	–0.2897	0.0045	170	4316.9050	–0.3029	0.0030
20	4246.1162	–0.2878	0.0026	171	4317.3694	–0.3174	–0.0046
21	4246.5864	–0.3196	0.0009	172	4317.8484	–0.3234	0.0025
22	4247.0586	–0.3165	0.0011	173	4318.3193	–0.3075	0.0015
23	4247.5308	–0.2958	0.0013	174	4318.7915	–0.2968	0.0018
24	4248.0059	–0.3138	0.0045	175	4319.2605	–0.3319	–0.0012
25	4248.4749	–0.3327	0.0016	176	4319.7356	–0.3056	0.0020
26	4248.9490	–0.3107	0.0038	177	4320.2078	–0.2931	0.0023
27	4249.4204	–0.3115	0.0033	178	4320.6777	–0.3057	0.0003
28	4249.8914	–0.3254	0.0023	179	4321.1499	–0.3289	0.0006
29	4250.3613	–0.3306	0.0004	180	4321.6282	–0.2922	0.0069
30	4250.8367	–0.3198	0.0038	181	4322.0920	–0.3153	–0.0012
31	4251.3047	–0.3351	–0.0001	182	4322.5652	–0.3069	0.0001
32	4251.7788	–0.3297	0.0021	183	4323.0403	–0.3153	0.0032
33	4252.2522	–0.3181	0.0036	184	4323.5112	–0.3005	0.0023
34	4252.7212	–0.3187	0.0006	185	4323.9815	–0.3187	0.0006
35	4253.1924	–0.3417	–0.0001	186	4324.4536	–0.3198	0.0008
36	4253.6655	–0.3186	0.0011	187	4324.9316	–0.3000	0.0069
37	4254.1375	–0.3269	0.0011	188	4325.3948	–0.3226	–0.0019
38	4254.6047	–0.3417	–0.0035	189	4325.8718	–0.3295	0.0033
39	4255.0808	–0.3360	0.0006	190	4326.3428	–0.3055	0.0023
40	4255.5510	–0.3204	–0.0011	191	4326.8140	–0.3040	0.0015
41	4256.0230	–0.3243	–0.0011	192	4327.2830	–0.3466	–0.0014
42	4256.4919	–0.3385	–0.0040	193	4327.7571	–0.3118	0.0008
43	4256.9724	–0.3264	0.0045	194	4328.2302	–0.3117	0.0020
44	4257.4365	–0.3199	–0.0033	195	4328.6973	–0.3270	–0.0028
45	4257.9136	–0.3298	0.0019	196	4329.1724	–0.3345	0.0003
46	4258.3826	–0.3174	–0.0011	197	4329.6475	–0.3096	0.0035
47	4258.8530	–0.3175	–0.0025	198	4330.1125	–0.3209	–0.0033
48	4259.3240	–0.3164	–0.0035	199	4330.5867	–0.3393	–0.0011
49	4259.8010	–0.3153	0.0016	200	4331.0588	–0.3096	–0.0009
50	4260.2703	–0.3012	–0.0011	201	4331.5337	–0.2995	0.0020
51	4260.7444	–0.3005	0.0011	202	4332.0019	–0.3159	–0.0016
52	4261.2146	–0.3120	–0.0006	203	4332.4749	–0.3266	–0.0006
53	4261.6899	–0.2990	0.0028	204	4332.9490	–0.2930	0.0016
54	4262.1587	–0.2893	–0.0003	205	4333.4202	–0.3034	0.0008
55	4262.6318	–0.3043	0.0009	206	4333.8892	–0.3261	–0.0021
56	4263.1050	–0.3056	0.0021	207	4334.3662	–0.3104	0.0030
57	4263.5791	–0.3029	0.0043	208	4334.8352	–0.2882	0.0001

Table 2. continued.

Cycle [E]	Times of maximum [HJD-2450000]	Magnitude	O–C [d]	Cycle [E]	Times of maximum [HJD-2450000]	Magnitude	O–C [d]
58	4264.0471	–0.3028	0.0004	209	4335.3103	–0.3210	0.0033
59	4264.5215	–0.3199	0.0028	210	4335.7776	–0.3119	–0.0014
60	4264.9954	–0.3087	0.0048	211	4336.2585	–0.2975	0.0077
61	4265.4658	–0.3106	0.0033	212	4336.7236	–0.3023	0.0008
62	4265.9358	–0.3246	0.0014	213	4337.1985	–0.2960	0.0038
63	4266.4131	–0.3258	0.0068	214	4337.6697	–0.3065	0.0030
64	4266.8801	–0.3175	0.0019	215	4338.1409	–0.3007	0.0023
65	4267.3501	–0.3299	–0.0001	216	4338.6108	–0.3005	0.0004
66	4267.8262	–0.3299	0.0041	217	4339.0862	–0.2863	0.0038
67	4268.2986	–0.3249	0.0046	218	4339.5559	–0.3066	0.0016
68	4268.7656	–0.3077	–0.0003	219	4340.0310	–0.2875	0.0048
69	4269.2427	–0.3302	0.0048	220	4340.5002	–0.3037	0.0021
70	4269.7126	–0.3390	0.0029	221	4340.9712	–0.2917	0.0011
71	4270.1858	–0.3101	0.0041	222	4341.4473	–0.2889	0.0053
72	4270.6531	–0.3371	–0.0005	223	4341.9175	–0.3070	0.0035
73	4271.1282	–0.3407	0.0026	224	4342.3852	–0.3147	–0.0006
74	4271.6013	–0.3368	0.0038	225	4342.8628	–0.2995	0.0050
75	4272.0684	–0.3376	–0.0010	226	4343.3315	–0.3275	0.0018
76	4272.5435	–0.3503	0.0021	227	4343.8008	–0.3282	–0.0009
77	4273.0137	–0.3427	0.0004	228	4344.2766	–0.3247	0.0031
78	4273.4856	–0.3354	0.0004	229	4344.7488	–0.3029	0.0033
79	4273.9539	–0.3491	–0.0032	230	4345.2161	–0.3364	–0.0013
80	4274.4290	–0.3353	0.0000	231	4345.6919	–0.3239	0.0026
81	4274.9001	–0.3355	–0.0008	232	4346.1650	–0.3162	0.0038
82	4275.3665	–0.3333	–0.0064	233	4346.6331	–0.3149	–0.0001
83	4275.8435	–0.3415	–0.0013	234	4347.1062	–0.3253	0.0011
84	4276.3203	–0.3182	0.0036	235	4347.5784	–0.3026	0.0014
85	4276.7856	–0.3190	–0.0030	236	4348.0503	–0.3075	0.0014
86	4277.2598	–0.3150	–0.0008	237	4348.5215	–0.3087	0.0006
87	4277.7339	–0.3124	0.0014	238	4348.9944	–0.3202	0.0016
88	4278.2031	–0.3145	–0.0013	239	4349.4675	–0.2917	0.0028
89	4278.6721	–0.3176	–0.0042	240	4349.9358	–0.3186	–0.0008
90	4279.1523	–0.3063	0.0041	241	4350.4087	–0.2909	0.0001
91	4279.6213	–0.3028	0.0012	242	4350.8818	–0.3119	0.0014
92	4280.0874	–0.3091	–0.0047	243	4351.3518	–0.2884	–0.0006
93	4280.5644	–0.3216	0.0004	244	4351.8259	–0.3056	0.0016
94	4281.0405	–0.3044	0.0046	245	4352.2949	–0.3014	–0.0013
95	4281.5068	–0.3080	–0.0010	246	4352.7739	–0.3039	0.0058
96	4281.9761	–0.3297	–0.0037	247	4353.2380	–0.2996	–0.0020
97	4282.4570	–0.3057	0.0053	248	4353.7141	–0.3066	0.0021
98	4282.9250	–0.3211	0.0014	249	4354.1863	–0.2979	0.0024
99	4283.3914	–0.3128	–0.0042	250	4354.6611	–0.2951	0.0053
100	4283.8684	–0.3320	0.0010	251	4355.1282	–0.2945	0.0004
101	4284.3433	–0.3093	0.0039	252	4355.6055	–0.2942	0.0058
102	4284.8106	–0.3158	–0.0008	253	4356.0745	–0.2756	0.0028
103	4285.2837	–0.3251	0.0005	254	4356.5464	–0.2858	0.0028
104	4285.7590	–0.3222	0.0039	255	4357.0156	–0.2945	0.0002
105	4286.2270	–0.3157	0.0000	256	4357.4951	–0.2857	0.0077
106	4286.6951	–0.3195	–0.0039	257	4357.9607	–0.2790	0.0014
107	4287.1699	–0.3237	–0.0010	258	4358.4358	–0.2837	0.0046
108	4287.6453	–0.3123	0.0024	259	4358.9048	–0.2916	0.0016
109	4288.1155	–0.3056	0.0007	260	4359.3784	–0.3010	0.0033
110	4288.5845	–0.3387	–0.0022	261	4359.8520	–0.2877	0.0051
111	4289.0606	–0.3156	0.0019	262	4360.3210	–0.3030	0.0021
112	4289.5298	–0.3262	–0.0007	263	4360.7952	–0.3060	0.0043
113	4290.0010	–0.3242	–0.0015	264	4361.2688	–0.3061	0.0060
114	4290.4749	–0.3425	0.0005	265	4361.7363	–0.3104	0.0016
115	4290.9470	–0.3333	0.0007	266	4362.2102	–0.3195	0.0036

Table 2. continued.

Cycle [E]	Times of maximum [HJD-2450000]	Magnitude	O–C [d]	Cycle [E]	Times of maximum [HJD-2450000]	Magnitude	O–C [d]
116	4291.4163	–0.3356	–0.0020	267	4362.6824	–0.3210	0.0038
117	4291.8882	–0.3453	–0.0020	268	4363.1555	–0.3195	0.0051
118	4292.3633	–0.3340	0.0012	269	4363.6216	–0.3224	–0.0008
119	4292.8335	–0.3353	–0.0005	270	4364.0984	–0.3280	0.0041
120	4293.3005	–0.3438	–0.0054	271	4364.5676	–0.3353	0.0014
121	4293.7817	–0.3115	0.0039	272	4365.0418	–0.3224	0.0036
122	4294.2498	–0.3288	0.0000	273	4365.5088	–0.3331	–0.0013
123	4294.7207	–0.3229	–0.0010	274	4365.9849	–0.3106	0.0029
124	4295.1931	–0.3282	–0.0005	275	4366.4539	–0.3248	–0.0001
125	4295.6692	–0.3057	0.0037	276	4366.9280	–0.3071	0.0021
126	4296.1331	–0.3142	–0.0044	277	4367.3980	–0.3096	0.0002
127	4296.6074	–0.3194	–0.0020	278	4367.8711	–0.3047	0.0014
128	4297.0815	–0.3070	0.0002	279	4368.3411	–0.3370	–0.0005
129	4297.5554	–0.3018	0.0022	280	4368.8142	–0.3108	0.0007
130	4298.0207	–0.3223	–0.0044	281	4369.2864	–0.3170	0.0009
131	4298.4968	–0.3127	–0.0002	282	4369.7617	–0.3135	0.0043
132	4298.9736	–0.2974	0.0046	283	4370.2273	–0.3188	–0.0020
133	4299.4380	–0.3152	–0.0029	284	4370.7043	–0.2918	0.0031
134	4299.9111	–0.3286	–0.0017	285	4371.1753	–0.3181	0.0021
135	4300.3899	–0.2974	0.0051	286	4371.6414	–0.2981	–0.0037
136	4300.8528	–0.2922	–0.0039	287	4372.1194	–0.3154	0.0024
137	4301.3232	–0.3135	–0.0054	288	4372.5916	–0.2918	0.0026
138	4301.8042	–0.3152	0.0037	289	4373.0647	–0.2853	0.0039
139	4302.2751	–0.3037	0.0027	290	4373.5308	–0.3080	–0.0020
140	4302.7415	–0.3143	–0.0029	291	4374.0107	–0.2919	0.0061
141	4303.2144	–0.3106	–0.0019	292	4374.4810	–0.2765	0.0044
142	4303.6917	–0.2957	0.0034	293	4374.9490	–0.2911	0.0004
143	4304.1616	–0.3063	0.0015	294	4375.4228	–0.2970	0.0024
144	4304.6328	–0.3113	0.0008	295	4375.8992	–0.2899	0.0068
145	4305.1047	–0.3109	0.0008	296	4376.3660	–0.2824	0.0017
146	4305.5779	–0.2979	0.0020	297	4376.8420	–0.3036	0.0058
147	4306.0440	–0.3199	–0.0039	298	4377.3123	–0.2884	0.0041
148	4306.5190	–0.3092	–0.0007	299	4377.7832	–0.2861	0.0031
149	4306.9951	–0.3014	0.0035	300	4378.2534	–0.2970	0.0014
150	4307.4644	–0.3171	0.0008	301	4378.7258	–0.3097	0.0019
151	4307.9333	–0.3326	–0.0022				